Temperature-dependent cross sections for $\pi\phi$ and $\rho\phi$ nonresonant reactions in hadronic matter*

LUO Zhi-Feng(罗志峰) XU Xiao-Ming(许晓明)[1)]

Department of Physics, Shanghai University, Shanghai 200444, China

Abstract: With a potential of which the large-distance part reflects lattice gauge results and of which the short-distance part is given by one gluon exchange plus perturbative one- and two-loop corrections, the Schrödinger equation brings about temperature dependence of meson masses and mesonic quark-antiquark relative-motion wave functions. The ground-state meson masses drop with increasing temperature. The transition amplitude calculated from the potential, the meson masses and the wave functions gives temperature-dependent cross sections for the five nonresonant reactions $\pi\phi \to K\bar{K}^*$ (or $K^*\bar{K}$), $\pi\phi \to K^*\bar{K}^*$, $\rho\phi \to K\bar{K}$, $\rho\phi \to K\bar{K}^*$ (or $K^*\bar{K}$) and $\rho\phi \to K^*\bar{K}^*$. The numerical temperature-dependent cross sections are parametrized. The peak cross section of either $\pi\phi \to K\bar{K}^*$ or $\pi\phi \to K^*\bar{K}^*$ increases from $T = 0$ to $T = 0.75T_c$ and decreases with further increasing temperature. The cross section for $\rho\phi \to K\bar{K}$, $\rho\phi \to K\bar{K}^*$ or $\rho\phi \to K^*\bar{K}^*$ has a decreasing trend while the temperature increases from $0.75T_c$.

Key words: meson-phi reaction, quark-interchange process, cross section

PACS: 25.75.-q, 13.75.Lb, 12.38.Mh **DOI:** 10.1088/1674-1137/36/9/008

1 Introduction

The ϕ meson is particular in relativistic heavy-ion collisions due to its hidden strange constituent quark and antiquark. The measurements on the ratios ϕ/π and Ω/ϕ [1–3] can be used to explore deconfinement by means of strangeness enhancement [4, 5]. The felicitous use of similar masses of phi and proton [6] gives a final identification on the scaling behavior of the elliptic flow over the constituent-quark number [7, 8]. The ϕ momentum spectra [3, 9–11] are used to find the in-medium modification of the hidden strangeness. Behind the observables is phi-involved physics: ϕ yield from s and $\bar{s}$ which are produced in parton-parton scattering in initial nucleus-nucleus collisions and deconfined matter; ϕ yield from hadron-hadron reactions and hadron decay in hadronic matter; ϕ absorption in hadronic matter; elastic parton-s scattering and elastic hadron-ϕ scattering that help establish thermalization of ϕ mesons. The ϕ absorption depends on hadronic matter and the absorption cross section is expected to depend on temperature. The ϕ absorption consists of resonant reactions, quark-antiquark annihilation processes where the gluon yielded in the annihilation produces a quark-antiquark pair in the lowest order, and reactions of which each is governed by a quark interchange. Quark-interchange processes which occur among pions, rhos, kaons and vector kaons have been shown to be important in the contribution of the inelastic meson-meson scattering to the evolution of mesonic matter [12]. We then expect that meson-phi quark-interchange processes are important in the ϕ absorption in mesonic matter and need to study the processes.

Effective meson Lagrangians in Refs. [13–15] offer small meson-phi cross sections, but the hidden local symmetry Lagrangian provides large collision rates of phis with rhos, kaons and vector kaons [16]. At the quark level the quark-interchange-induced reactions $\pi\phi \to K\bar{K}^*+K^*\bar{K}+K^*\bar{K}^*$ and $\rho\phi \to K\bar{K}+K\bar{K}^*+K^*\bar{K}+K^*\bar{K}^*$ were studied [17] in the quark-interchange mechanism [18]. In the above studies the meson-phi reactions are placed in vacuum. Since the realistic phi mesons are one species of hadronic matter, the above work should be developed to study in-medium

Received 15 November 2011

* Supported by National Natural Science Foundation of China (11175111)

1) E-mail: xmxu@mail.shu.edu.cn

modification of meson-phi reactions. Temperature dependence of the meson-phi quark-interchange processes is not known in experiments or theory. Therefore, we study the temperature dependence of cross sections for the processes in this work.

Since the two constituents of the π(ρ) meson and those of the ϕ meson do not have the same flavor, the quark-antiquark annihilation does not happen in the πϕ and ρϕ reactions. The πϕ and ρϕ nonresonant reactions are only governed by the quark interchange. The quark-interchange mechanism is thus used in this work to study the temperature dependence of cross sections for the quark-interchange-induced reactions $\pi\phi \to K\bar{K}^*$ (or $K^*\bar{K}$), $\pi\phi \to K^*\bar{K}^*$, $\rho\phi \to K\bar{K}$, $\rho\phi \to K\bar{K}^*$ (or $K^*\bar{K}$) and $\rho\phi \to K^*\bar{K}^*$. These reactions are important in the ϕ absorption in hadronic matter produced in Au-Au collisions at the Relativistic Heavy Ion Collider since the dominant species of hadronic matter are π and ρ. We establish the notation $\mathrm{K} = \begin{pmatrix} \mathrm{K}^+ \\ \mathrm{K}^0 \end{pmatrix}$ and $\bar{\mathrm{K}} = \begin{pmatrix} \bar{\mathrm{K}}^0 \\ \mathrm{K}^- \end{pmatrix}$ for the pseudoscalar isospin doublets as well as $\mathrm{K}^* = \begin{pmatrix} \mathrm{K}^{*+} \\ \mathrm{K}^{*0} \end{pmatrix}$ and $\bar{\mathrm{K}}^* = \begin{pmatrix} \bar{\mathrm{K}}^{*0} \\ \mathrm{K}^{*-} \end{pmatrix}$ for the vector isospin doublets.

In the next section we introduce a method for obtaining cross sections for meson-meson nonresonant reactions governed by the quark interchange. In Section 3 numerical results of cross sections and discussions are shown. Parametrizations of the numerical cross sections are offered. A summary is in the last section. Temperature-dependent masses of ϕ and η mesons are presented in Appendix A and how to use the cross sections obtained in the method is in Appendix B.

2 Method for obtaining cross sections

Each of the πϕ and ρϕ reactions is governed by one quark interchange. The reactions which occur in vacuum have been studied in the Born approximation in Ref. [17]. The reactions which occur at finite temperatures, with which we are concerned in this work, are still studied in the Born approximation. In this approximation we arrive at temperature dependence of the cross sections for the reactions while this approximation needs temperature dependence of a quark potential, mesonic quark-antiquark relative-motion wave functions and meson masses. The potential, wave functions and masses are first described in this section. Based on them, we show transition amplitudes and the cross sections.

We obtained the following central spin-independent potential of constituents a and b in Ref. [19],

$$V_{\mathrm{si}}(\vec{r}) = -\frac{\vec{\lambda}_{\mathrm{a}}}{2}\cdot\frac{\vec{\lambda}_{\mathrm{b}}}{2}\frac{3}{4}D\left[1.3-\left(\frac{T}{T_{\mathrm{c}}}\right)^4\right]\tanh(Ar) + \frac{\vec{\lambda}_a}{2}\cdot\frac{\vec{\lambda}_b}{2}\frac{6\pi}{25}\frac{v(\lambda r)}{r}\exp(-Er), \quad (1)$$

where the critical temperature $T_{\mathrm{c}} = 0.175$ GeV, $\lambda = \sqrt{3b_0/16\pi^2\alpha'}$ with $b_0 = 25/3$ and $\alpha' = 1.04\ \mathrm{GeV}^{-2}$, $\vec{\lambda}_{\mathrm{a}}$ are the Gell-Mann matrices for the color generators and the dimensionless function v is given by

$$v(x) = \frac{4b_0}{\pi}\int_0^\infty \frac{\mathrm{d}Q}{Q}\left(\rho(\vec{Q}^2) - \frac{K}{\vec{Q}^2}\right)\sin\left(\frac{Q}{\lambda}x\right), \quad (2)$$

where $K = 3/16\pi^2\alpha'$ only in this integrand, the quantity $\rho - \dfrac{K}{\vec{Q}^2}$ arises from one-gluon exchange and perturbative one- and two-loop corrections, Q is the absolute value of gluon momentum $\vec{Q}$ and $\rho(\vec{Q}^2)$ is given by Buchmüller and Tye [20]. Only in this potential

$$A = 1.5\left[0.75 + 0.25\left(\frac{T}{T_{\mathrm{c}}}\right)^{10}\right]^6\ \mathrm{GeV},$$

$D = 0.7$ GeV and $E = 0.6$ GeV. The potential is valid for a temperature T smaller than T_{c}. When the constituent-constituent distance r approaches zero, the potential comes from one-gluon exchange plus perturbative one- and two-loop corrections. At large distances the potential becomes a constant that relies on temperature and was given by the lattice calculations in Ref. [21]. The lattice calculations offered the numerical quark potential at intermediate and large distances, which was individually parametrized by Wong [22] and Digal et al. [23] with different functions of r and T.

We obtain meson masses by first using the central spin-independent potential in the Schrödinger equation and then using the spin-spin interaction that arises from one-gluon exchange and perturbative one- and two-loop corrections [24]

$$V_{\mathrm{ss}}(\vec{r}) = -\frac{\vec{\lambda}_{\mathrm{a}}}{2}\cdot\frac{\vec{\lambda}_{\mathrm{b}}}{2}\frac{16\pi^2}{25}\delta^3(\vec{r})\frac{\vec{s}_{\mathrm{a}}\cdot\vec{s}_{\mathrm{b}}}{m_{\mathrm{a}}m_{\mathrm{b}}} + \frac{\vec{\lambda}_{\mathrm{a}}}{2}\cdot\frac{\vec{\lambda}_{\mathrm{b}}}{2}\frac{4\pi}{25}\frac{1}{r}\frac{\mathrm{d}^2v(\lambda r)}{\mathrm{d}r^2}\frac{\vec{s}_{\mathrm{a}}\cdot\vec{s}_{\mathrm{b}}}{m_{\mathrm{a}}m_{\mathrm{b}}}, \quad (3)$$

where $\vec{s}_{\mathrm{a}}$ (m_{a}) is the spin (mass) of the constituent quark or antiquark labeled as a. Vacuum masses of pion, rho, kaon and vector kaon and temperature-dependent masses of the four mesons have already

been obtained in Ref. [19] with an up or down quark mass of 0.32 GeV and a strange quark mass of 0.5 GeV. In Appendix A we show how to obtain the vacuum masses of ϕ and η and temperature-dependent masses of the two mesons.

The Schrödinger equation with the central spin-independent potential is solved to obtain the wave functions of quark-antiquark relative motion in mesons. With the wave functions, the potential and the meson masses, we calculate the transition amplitude $\mathcal{M}_{\rm fi}$ for a reaction governed by one quark interchange in the Born approximation. The reaction $\mathrm{A}(\mathrm{q}_1\overline{\mathrm{q}}_1)+\mathrm{B}(\mathrm{q}_2\overline{\mathrm{q}}_2)\to\mathrm{C}(\mathrm{q}_1\overline{\mathrm{q}}_2)+\mathrm{D}(\mathrm{q}_2\overline{\mathrm{q}}_1)$ of mesons A and B has two forms, the prior form and the post form [25–27]. Gluon propagation between two constituents takes place before the quark interchange in the prior form or after the quark interchange in the post form. The transition amplitude in the prior form is [17]

$$\mathcal{M}_{\rm fi}^{\rm prior}=\sqrt{2E_{\mathrm{q}_1\bar{\mathrm{q}}_1}2E_{\mathrm{q}_2\bar{\mathrm{q}}_2}2E_{\mathrm{q}_1\bar{\mathrm{q}}_2}2E_{\mathrm{q}_2\bar{\mathrm{q}}_1}}\int\frac{\mathrm{d}^3p_{\mathrm{q}_1\bar{\mathrm{q}}_2}}{(2\pi)^3}\frac{\mathrm{d}^3p_{\mathrm{q}_2\bar{\mathrm{q}}_1}}{(2\pi)^3}\times\psi^+_{\mathrm{q}_1\bar{\mathrm{q}}_2}(\vec{p}_{\mathrm{q}_1\bar{\mathrm{q}}_2})\psi^+_{\mathrm{q}_2\bar{\mathrm{q}}_1}(\vec{p}_{\mathrm{q}_2\bar{\mathrm{q}}_1})(V_{\mathrm{q}_1\bar{\mathrm{q}}_2}+V_{\bar{\mathrm{q}}_1\mathrm{q}_2}$$
$$+V_{\mathrm{q}_1\mathrm{q}_2}+V_{\bar{\mathrm{q}}_1\bar{\mathrm{q}}_2})\psi_{\mathrm{q}_1\bar{\mathrm{q}}_1}(\vec{p}_{\mathrm{q}_1\bar{\mathrm{q}}_1})\psi_{\mathrm{q}_2\bar{\mathrm{q}}_2}(\vec{p}_{\mathrm{q}_2\bar{\mathrm{q}}_2}),\tag{4}$$

and the transition amplitude in the post form is

$$\begin{aligned}\mathcal{M}_{\rm fi}^{\rm post}=\sqrt{2E_{\mathrm{q}_1\bar{\mathrm{q}}_1}2E_{\mathrm{q}_2\bar{\mathrm{q}}_2}2E_{\mathrm{q}_1\bar{\mathrm{q}}_2}2E_{\mathrm{q}_2\bar{\mathrm{q}}_1}}\Bigg(&\int\frac{\mathrm{d}^3p_{\mathrm{q}_1\bar{\mathrm{q}}_1}}{(2\pi)^3}\frac{\mathrm{d}^3p_{\mathrm{q}_1\bar{\mathrm{q}}_2}}{(2\pi)^3}\psi^+_{\mathrm{q}_1\bar{\mathrm{q}}_2}(\vec{p}_{\mathrm{q}_1\bar{\mathrm{q}}_2})\psi^+_{\mathrm{q}_2\bar{\mathrm{q}}_1}(\vec{p}_{\mathrm{q}_2\bar{\mathrm{q}}_1})V_{\mathrm{q}_1\bar{\mathrm{q}}_1}\psi_{\mathrm{q}_1\bar{\mathrm{q}}_1}(\vec{p}_{\mathrm{q}_1\bar{\mathrm{q}}_1})\psi_{\mathrm{q}_2\bar{\mathrm{q}}_2}(\vec{p}_{\mathrm{q}_2\bar{\mathrm{q}}_2})\\&+\int\frac{\mathrm{d}^3p_{\mathrm{q}_2\bar{\mathrm{q}}_2}}{(2\pi)^3}\frac{\mathrm{d}^3p_{\mathrm{q}_2\bar{\mathrm{q}}_1}}{(2\pi)^3}\psi^+_{\mathrm{q}_1\bar{\mathrm{q}}_2}(\vec{p}_{\mathrm{q}_1\bar{\mathrm{q}}_2})\psi^+_{\mathrm{q}_2\bar{\mathrm{q}}_1}(\vec{p}_{\mathrm{q}_2\bar{\mathrm{q}}_1})V_{\bar{\mathrm{q}}_2\mathrm{q}_2}\psi_{\mathrm{q}_1\bar{\mathrm{q}}_1}(\vec{p}_{\mathrm{q}_1\bar{\mathrm{q}}_1})\psi_{\mathrm{q}_2\bar{\mathrm{q}}_2}(\vec{p}_{\mathrm{q}_2\bar{\mathrm{q}}_2})\\&+\int\frac{\mathrm{d}^3p_{\mathrm{q}_1\bar{\mathrm{q}}_2}}{(2\pi)^3}\frac{\mathrm{d}^3p_{\mathrm{q}_2\bar{\mathrm{q}}_1}}{(2\pi)^3}\psi^+_{\mathrm{q}_1\bar{\mathrm{q}}_2}(\vec{p}_{\mathrm{q}_1\bar{\mathrm{q}}_2})\psi^+_{\mathrm{q}_2\bar{\mathrm{q}}_1}(\vec{p}_{\mathrm{q}_2\bar{\mathrm{q}}_1})V_{q_1q_2}\psi_{\mathrm{q}_1\bar{\mathrm{q}}_1}(\vec{p}_{\mathrm{q}_1\bar{\mathrm{q}}_1})\psi_{\mathrm{q}_2\bar{\mathrm{q}}_2}(\vec{p}_{\mathrm{q}_2\bar{\mathrm{q}}_2})\\&+\int\frac{\mathrm{d}^3p_{\mathrm{q}_1\bar{\mathrm{q}}_2}}{(2\pi)^3}\frac{\mathrm{d}^3p_{\mathrm{q}_2\bar{\mathrm{q}}_1}}{(2\pi)^3}\psi^+_{\mathrm{q}_1\bar{\mathrm{q}}_2}(\vec{p}_{\mathrm{q}_1\bar{\mathrm{q}}_2})\psi^+_{\mathrm{q}_2\bar{\mathrm{q}}_1}(\vec{p}_{\mathrm{q}_2\bar{\mathrm{q}}_1})V_{\bar{q}_1\bar{q}_2}\psi_{\mathrm{q}_1\bar{\mathrm{q}}_1}(\vec{p}_{\mathrm{q}_1\bar{\mathrm{q}}_1})\psi_{\mathrm{q}_2\bar{\mathrm{q}}_2}(\vec{p}_{\mathrm{q}_2\bar{\mathrm{q}}_2})\Bigg).\end{aligned}\tag{5}$$

The transition amplitude in the prior or post form depends on the energies, $E_{\mathrm{q}_1\overline{\mathrm{q}}_1}$, $E_{\mathrm{q}_2\overline{\mathrm{q}}_2}$, $E_{\mathrm{q}_1\overline{\mathrm{q}}_2}$ and $E_{\mathrm{q}_2\overline{\mathrm{q}}_1}$, of the four mesons, the quark-antiquark relative-motion wave functions $\psi_{\rm ab}$ versus the relative momenta $\vec{p}_{ab}$ and the potential $V_{\rm ab}$ of constituents a and b. It is not obvious that $\mathcal{M}_{\rm fi}^{\rm prior}=\mathcal{M}_{\rm fi}^{\rm post}$ can be derived from Eqs. (4) and (5) but indeed $\mathcal{M}_{\rm fi}^{\rm prior}=\mathcal{M}_{\rm fi}^{\rm post}$ if the wave functions $\psi_{\rm ab}$ of mesons are solutions of the Schrödinger equation with $V_{\rm ab}$ [25–27]. The so-called post-prior discrepancy $\mathcal{M}_{\rm fi}^{\rm prior}\neq\mathcal{M}_{\rm fi}^{\rm post}$ occurs while the wave functions do not satisfy the Schrödinger equation with $V_{\rm ab}$. Eqs. (4) and (5) display the transition amplitudes in momentum space. This needs the quark potential as a function of the gluon momentum, which is the Fourier transform of $V_{\rm si}(\vec{r})+V_{\rm ss}(\vec{r})$,

$$\begin{aligned}V_{\rm ab}\left(\vec{Q}\right)=&-\frac{\vec{\lambda}_{\rm a}}{2}\cdot\frac{\vec{\lambda}_{\rm b}}{2}\frac{3}{4}D\left[1.3-\left(\frac{T}{T_{\rm c}}\right)^4\right]\left[(2\pi)^3\delta^3(\vec{Q})-\frac{8\pi}{Q}\int_0^\infty\mathrm{d}r\frac{r\sin(Qr)}{\exp(2Ar)+1}\right]\\&+\frac{\vec{\lambda}_{\rm a}}{2}\cdot\frac{\vec{\lambda}_{\rm b}}{2}64\pi E\int_0^\infty\mathrm{d}q\frac{\rho(q^2)-\frac{K}{q^2}}{(E^2+Q^2+q^2)^2-4Q^2q^2}-\frac{\vec{\lambda}_{\rm a}}{2}\cdot\frac{\vec{\lambda}_{\rm b}}{2}\frac{16\pi^2}{25}\frac{\vec{s}_{\rm a}\cdot\vec{s}_{\rm b}}{m_{\rm a}m_{\rm b}}\\&+\frac{\vec{\lambda}_{\rm a}}{2}\cdot\frac{\vec{\lambda}_{\rm b}}{2}\frac{16\pi^2\lambda}{25Q}\int_0^\infty\mathrm{d}x\frac{\mathrm{d}^2v(x)}{\mathrm{d}x^2}\sin\left(\frac{Q}{\lambda}x\right)\frac{\vec{s}_{\rm a}\cdot\vec{s}_{\rm b}}{m_{\rm a}m_{\rm b}}.\end{aligned}\tag{6}$$

Now the potential $V_{\rm ab}$ contains both the central spin-independent potential and the spin-spin interaction. Hence, the wave functions $\psi_{\rm ab}$ which are the Fourier transform of the relative-motion wave functions determined by the central spin-independent potential $V_{\rm si}$ are not solutions of the Schrödinger equation with $V_{\rm ab}$, and the post-prior discrepancy takes place in our calculations. Related to the scattering in the prior form and in the post form, we get two cross sections [17]

$$\sigma^{\rm prior}=\frac{1}{32\pi s}\frac{|\vec{P}'(\sqrt{s})|}{|\vec{P}(\sqrt{s})|}\int_0^\pi\mathrm{d}\theta|\mathcal{M}_{\rm fi}^{\rm prior}(s,t)|^2\sin\theta,\tag{7}$$

and

$$\sigma^{\rm post}=\frac{1}{32\pi s}\frac{|\vec{P}'(\sqrt{s})|}{|\vec{P}(\sqrt{s})|}\int_0^\pi\mathrm{d}\theta|\mathcal{M}_{\rm fi}^{\rm post}(s,t)|^2\sin\theta,\tag{8}$$

which lead to the polarized cross section

$$\sigma = \frac{\sigma^{\rm prior} + \sigma^{\rm post}}{2}. \quad (9)$$

In Eqs. (7) and (8) the Mandelstam variables are $s = (E_{\rm q_1\bar{q}_1} + E_{\rm q_2\bar{q}_2})^2 - (\vec{P}_{\rm q_1\bar{q}_1} + \vec{P}_{\rm q_2\bar{q}_2})^2$ and $t = (E_{\rm q_1\bar{q}_1} - E_{\rm q_1\bar{q}_2})^2 - (\vec{P}_{\rm q_1\bar{q}_1} - \vec{P}_{\rm q_1\bar{q}_2})^2$ where the mesons A, B, C and D have the momenta $\vec{P}_{\rm q_1\bar{q}_1}$, $\vec{P}_{\rm q_2\bar{q}_2}$, $\vec{P}_{\rm q_1\bar{q}_2}$ and $\vec{P}_{\rm q_2\bar{q}_1}$, respectively. In the center-of-mass frame the mesons A, B, C and D have the momenta $\vec{P}$, $-\vec{P}$, $\vec{P}'$ and $-\vec{P}'$, respectively. θ is the angle between $\vec{P}$ and $\vec{P}'$.

The unpolarized cross section for $\rm A(q_1\overline{q}_1) + B(q_2\overline{q}_2) \to C(q_1\overline{q}_2) + D(q_2\overline{q}_1)$ is

$$\sigma^{\rm unpol}(\sqrt{s}, T) = \frac{1}{(2S_{\rm A}+1)(2S_{\rm B}+1)} \sum_S (2S+1)\sigma(S, m_{\rm S}, \sqrt{s}), \quad (10)$$

where $S_{\rm A}$, $S_{\rm B}$ and S are the spin of A, the spin of B and the total spin of the two mesons, respectively. The unpolarized cross section does not depend on the magnetic projection quantum number $m_{\rm S}$ of S.

3 Numerical results and discussions

A quark-interchange-induced reaction may be an endothermic reaction which has the general features: (1) the threshold energy equals the sum of the masses of the two final mesons; (2) the cross section is zero at the threshold energy or at $\sqrt{s} \to \infty$; (3) the cross section has a maximum, i.e. a peak cross section. While temperature changes, the threshold energy and the peak cross section change. When the distance r between the quark and the antiquark in a meson is large enough, the central spin-independent potential at a given temperature exhibits a constant value and becomes a plateau. The value decreases with increasing temperature and this means confinement gets weaker. Solutions of the Schrödinger equation with the potential show that the meson's root-mean-square radius increases and any bound state becomes looser and looser. Cross sections increase with increasing radii of initial mesons but decrease with weakening final bound states. When temperature increases, the two factors generate rising or falling peak cross sections. Indeed, this anticipation is confirmed by the temperature dependence of the unpolarized cross sections for the two nonresonant reactions, $\pi\phi \to \rm K\bar{K}^*$ in Fig. 1 and $\pi\phi \to \rm K^*\bar{K}^*$ in Fig. 2. Each curve in the two figures exhibits one or two peaks. In the following we refer the peak to that high peak if two peaks appear. While temperature goes up from zero, the peak cross section increases. At $T \to T_{\rm c}$ the peak cross section decreases. The maximum of the peak cross section is located at $T/T_{\rm c} = 0.75$ and has the value 2.72 mb for $\pi\phi \to \rm K\bar{K}^*$ or 0.84 mb for $\pi\phi \to \rm K^*\bar{K}^*$. Given a temperature, the peak cross section for $\pi\phi \to \rm K\bar{K}^*$ is larger than that for $\pi\phi \to \rm K^*\bar{K}^*$.

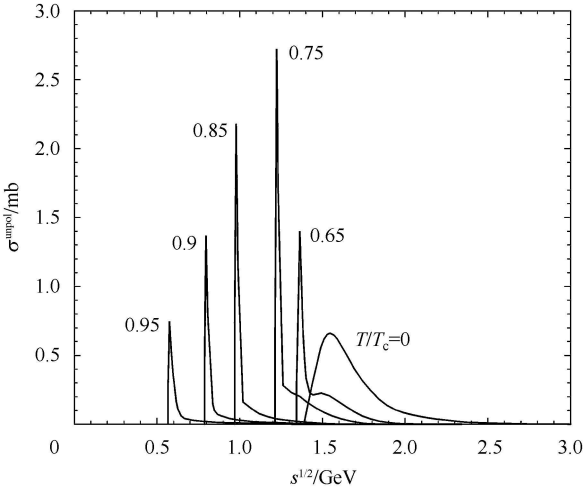

Fig. 1. $\pi\phi \to \rm K\bar{K}^*$ cross sections at various temperatures.

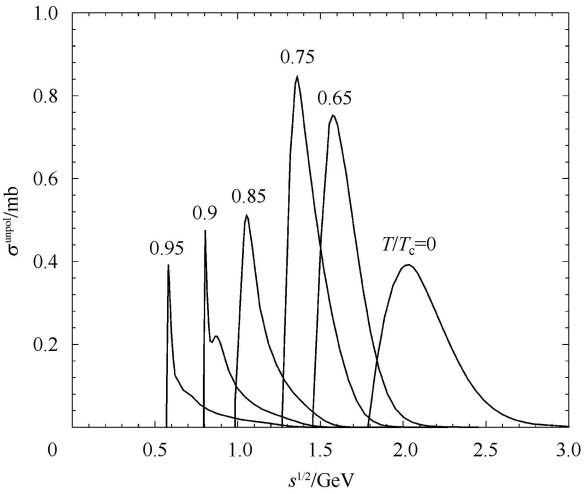

Fig. 2. $\pi\phi \to \rm K^*\bar{K}^*$ cross sections at various temperatures.

The numerical cross sections for the πϕ reactions are parametrized as

$$\sigma^{\rm unpol}(\sqrt{s}, T) = a_1 \left(\frac{\sqrt{s} - \sqrt{s_0}}{b_1}\right)^{c_1} \times \exp\left[c_1\left(1 - \frac{\sqrt{s} - \sqrt{s_0}}{b_1}\right)\right] + a_2 \left(\frac{\sqrt{s} - \sqrt{s_0}}{b_2}\right)^{c_2} \times \exp\left[c_2\left(1 - \frac{\sqrt{s} - \sqrt{s_0}}{b_2}\right)\right]. \quad (11)$$

Table 1. Values of parameters in the parametrization given in Eq. (11) for the reaction $\pi\phi \to K\bar{K}^*$. a_1 and a_2 are in units of mb; b_1, b_2, d_0 and $\sqrt{s_z}$ are in units of GeV; c_1 and c_2 are dimensionless.

T/T_c	a_1	b_1	c_1	a_2	b_2	c_2	d_0	$\sqrt{s_z}$
0	0.01	0.01	0.2	0.63	0.16	1.55	0.16	2.597
0.65	0.21	0.09	0.01	1.59	0.01	0.8	0.02	1.885
0.75	0.6	0.001	0.02	2.15	0.01	1.62	0.01	1.652
0.85	0.67	0.001	0.03	1.76	0.01	3.14	0.01	1.339
0.9	0.6	0.003	0.11	0.85	0.01	2.48	0.01	1.175
0.95	0.22	0.001	0.02	0.52	0.01	0.83	0.01	1.109

Table 2. The same as Table 1 except for $\pi\phi \to K^*\bar{K}^*$.

T/T_c	a_1	b_1	c_1	a_2	b_2	c_2	d_0	$\sqrt{s_z}$
0	0.01	0.001	0.93	0.39	0.21	1.46	0.25	2.926
0.65	0.02	0.001	0.01	0.77	0.13	1.74	0.12	2.095
0.75	0.02	0.002	0.01	0.79	0.1	1.22	0.09	1.853
0.85	0.05	0.015	0.01	0.43	0.06	0.81	0.07	1.593
0.9	0.47	0.004	0.6	0.22	0.05	0.43	0.01	1.44
0.95	0.1	0.02	0.06	0.29	0.01	0.96	0.01	1.296

Values of the parameters, a_1, b_1, c_1, a_2, b_2 and c_2, are listed in Table 1 for $\pi\phi \to K\bar{K}^*$ and in Table 2 for $\pi\phi \to K^*\bar{K}^*$. The cross section for $\pi\phi \to K^*\bar{K}$ equals the one for $\pi\phi \to K\bar{K}^*$.

We denote by $\sqrt{s_{\rm p}}$ the square root of the Mandelstam variable corresponding to the peak cross section. In the two tables we show the difference of $\sqrt{s_{\rm p}}$ with respect to the threshold energy $\sqrt{s_0}$, $d_0 = \sqrt{s_{\rm p}} - \sqrt{s_0}$. d_0 indicates sensitivity of a reaction to the energy variation with respect to the threshold energy. The smaller the d_0, the more sensitive a reaction. Since the masses of kaon and vector kaon decrease with increasing temperature [19], the threshold energy decreases as shown in Figs. 1 and 2. Not only $\sqrt{s_0}$ decreases, but also $\sqrt{s_{\rm p}}$ decreases. However, d_0 first decreases with increasing temperature and then arrives at 0.01 independent of temperature. In Tables 1 and 2 we list $\sqrt{s_z}$ that is the square root of the Mandelstam variable at which the cross section is 1/100 of the peak cross section. The open interval ($\sqrt{s_0}$, $\sqrt{s_z}$) indicates the energy region where a reaction effectively takes place.

Due to the mass difference of π and ρ, the $\pi\phi$ reactions are endothermic and the $\rho\phi$ reactions are exothermic. We plot unpolarized cross sections for the three nonresonant reactions $\rho\phi \to K\bar{K}$, $\rho\phi \to K\bar{K}^*$ and $\rho\phi \to K^*\bar{K}^*$ in Figs. 3–5, respectively. The numerical cross sections for the $\rho\phi$ reactions are parametrized as

$$\begin{aligned}\sigma^{\rm unpol}(\sqrt{s},T) = {} & \frac{\vec{P}'^2}{\vec{P}^2}\left\{a_1\left(\frac{\sqrt{s}-\sqrt{s_0}}{b_1}\right)^{c_1}\right. \\ & \times\exp\left[c_1\left(1-\frac{\sqrt{s}-\sqrt{s_0}}{b_1}\right)\right] \\ & +a_2\left(\frac{\sqrt{s}-\sqrt{s_0}}{b_2}\right)^{c_2} \\ & \left.\times\exp\left[c_2\left(1-\frac{\sqrt{s}-\sqrt{s_0}}{b_2}\right)\right]\right\}, \quad (12)\end{aligned}$$

where

$$\vec{P}^2 = \frac{1}{4s}\left\{\left[s-\left(m^2_{q_1\bar{q}_1}+m^2_{q_2\bar{q}_2}\right)\right]^2-4m^2_{q_1\bar{q}_1}m^2_{q_2\bar{q}_2}\right\}, \quad (13)$$

$$\vec{P}'^2 = \frac{1}{4s}\left\{\left[s-\left(m^2_{q_1\bar{q}_2}+m^2_{q_2\bar{q}_1}\right)\right]^2-4m^2_{q_1\bar{q}_2}m^2_{q_2\bar{q}_1}\right\}, \quad (14)$$

in which $m_{q_1\bar{q}_1}$, $m_{q_2\bar{q}_2}$, $m_{q_1\bar{q}_2}$ and $m_{q_2\bar{q}_1}$ are the masses of mesons $A(q_1\bar{q}_1)$, $B(q_2\bar{q}_2)$, $C(q_1\bar{q}_2)$ and $D(q_2\bar{q}_1)$, respectively. Values of the parameters, a_1, b_1, c_1, a_2, b_2 and c_2, are listed in Tables 3–5 for $\rho\phi \to K\bar{K}$, $\rho\phi \to K\bar{K}^*$ and $\rho\phi \to K^*\bar{K}^*$, respectively. The cross section for $\rho\phi \to K^*\bar{K}$ equals the one for $\rho\phi \to K\bar{K}^*$. For the quantity enclosed by the braces we list d_0 and $\sqrt{s_z}$ in Tables 3–5. $\sqrt{s_0}$ is the sum of the masses of ρ and ϕ mesons. d_0 decreases with

Table 3. Values of parameters in the parametrization given in Eq. (12) for the reaction $\rho\phi \to K\bar{K}$. a_1 and a_2 are in units of mb; b_1, b_2, d_0 and $\sqrt{s_z}$ are in units of GeV; c_1 and c_2 are dimensionless.

T/T_c	a_1	b_1	c_1	a_2	b_2	c_2	d_0	$\sqrt{s_z}$
0	0.01	0.14	0.66	0.02	0.19	2.14	0.2	2.648
0.65	0.008	0.008	0.53	0.05	0.15	1.93	0.15	2.103
0.75	0.015	0.004	0.61	0.07	0.12	1.7	0.1	1.854
0.85	0.025	0.004	0.43	0.057	0.084	2.61	0.08	1.597
0.9	0.023	0.086	1.1	0.07	0.005	0.5	0.005	1.433
0.95	0.05	0.006	0.54	0.01	0.06	0.32	0.005	1.305

Table 4. The same as Table 3 except for $\rho\phi \to K\bar{K}^*$.

T/T_c	a_1	b_1	c_1	a_2	b_2	c_2	d_0	$\sqrt{s_z}$
0	0.003	0.001	0.01	0.14	0.17	1.04	0.2	2.837
0.65	0.038	0.007	0.51	0.29	0.12	1.59	0.1	2.074
0.75	0.011	0.82	0.3	0.23	0.09	2.99	0.08	1.839
0.85	0.04	0.0034	0.5	0.14	0.08	1.59	0.07	1.592
0.9	0.038	0.005	1.65	0.07	0.02	0.13	0.005	1.46
0.95	0.04	0.006	0.84	0.03	0.03	0.19	0.005	1.336

Table 5. The same as Table 3 except for $\rho\phi \to K^*\bar{K}^*$.

T/T_c	a_1	b_1	c_1	a_2	b_2	c_2	d_0	$\sqrt{s_z}$
0	0.04	0.003	0.5	1.06	0.18	1.3	0.15	2.859
0.65	4	0.005	0.44	1.5	0.11	1.95	0.005	1.99
0.75	4.16	0.004	0.36	1.21	0.09	4.01	0.005	1.751
0.85	0.74	0.002	0.23	0.47	0.01	0.05	0.001	1.532
0.9	0.39	0.001	0.19	0.44	0.01	0.31	0.001	1.413
0.95	0.21	0.002	0.29	0.14	0.02	0.26	0.001	1.334

increasing temperature and approaches 0.005 for $\rho\phi \to K\bar{K}$ and $\rho\phi \to K\bar{K}^*$ or 0.001 for $\rho\phi \to K^*\bar{K}^*$. Hence, at a higher temperature the reactions are generally more sensitive to the energy variation with respect to the threshold energy.

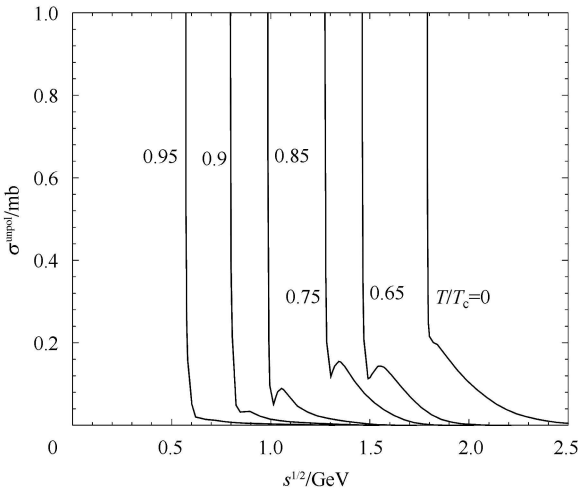

Fig. 3. $\rho\phi \to K\bar{K}$ cross sections at various temperatures.

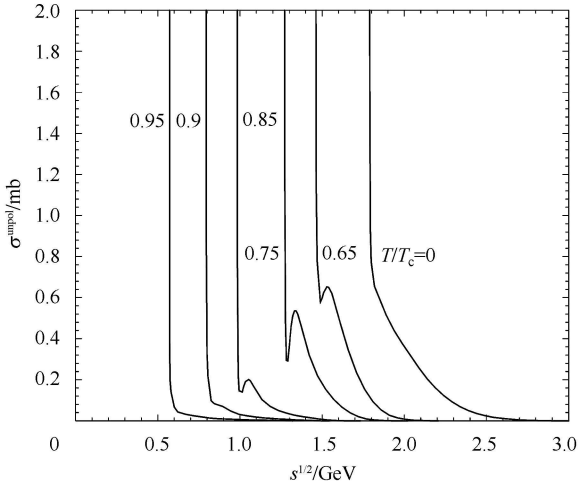

Fig. 4. $\rho\phi \to K\bar{K}^*$ cross sections at various temperatures.

In the exothermic reactions ρ and ϕ have momenta $\vec{P} = 0$ and the final mesons have $\vec{P}' \neq 0$ in the center-of-mass frame at the threshold energies. For a reaction at a given temperature a very small increase of $\sqrt{s}$ from the threshold energy $\sqrt{s_0}$

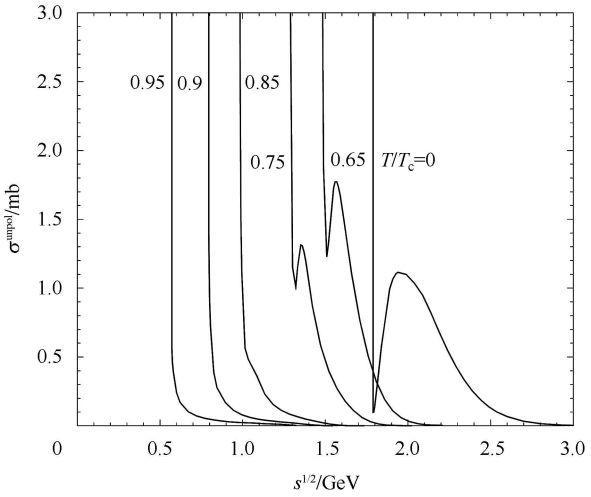

Fig. 5. $\rho\phi \to K^*\bar{K}^*$ cross sections at various temperatures.

causes a very rapid decrease in $\vec{P}'^2/\vec{P}^2$. Since d_0 for $\rho\phi \to K\bar{K}$ at T/T_c =0, 0.65, 0.75, 0.85 ($\rho\phi \to K\bar{K}^*$ at T/T_c =0, 0.65, 0.75, 0.85; $\rho\phi \to K^*\bar{K}^*$ at T/T_c =0, 0.65, 0.75) are much larger than d_0 at T/T_c =0.9, 0.95 (at T/T_c =0.9, 0.95; at T/T_c =0.85, 0.9, 0.95), we say that the quantity enclosed by the braces in Eq. (12) for the former increases slowly from the threshold energy and the quantity for the latter increases rapidly. If the quantity increases slowly and is overcome in part by the decrease of $\vec{P}'^2/\vec{P}^2$, one peak cross section appears like the curve at $T/T_c = 0.65$, 0.75 or 0.85 excluding $\rho\phi \to K^*\bar{K}^*$. If the quantity increases rapidly to a small value and is completely overcome by the decrease of $\vec{P}'^2/\vec{P}^2$, no peak cross section appears like the curve at $T/T_c = 0.9$, 0.95 or 0.85 only for $\rho\phi \to K^*\bar{K}^*$. The experimental mass of vector kaon is 1.8 times the one of kaon. $\vec{P}'^2/\vec{P}^2$ for $\rho\phi \to K\bar{K}$, $\rho\phi \to K\bar{K}^*$ and $\rho\phi \to K^*\bar{K}^*$ are in decreasing order. The decrease of $\vec{P}'^2/\vec{P}^2$ for $\rho\phi \to K\bar{K}$ or $\rho\phi \to K\bar{K}^*$ can overcome the increase of the quantity but the one for $\rho\phi \to K^*\bar{K}^*$ can not. Hence, no peak cross section appears like the curve at $T/T_c = 0$ for $\rho\phi \to K\bar{K}$ or $\rho\phi \to K\bar{K}^*$, or a wide peak appears like the curve at $T/T_c = 0$ for $\rho\phi \to K^*\bar{K}^*$. At $T = 0.65T_c$ or $T = 0.75T_c$ the peak cross sections for $\rho\phi \to K\bar{K}$, $\rho\phi \to K\bar{K}^*$ and $\rho\phi \to K^*\bar{K}^*$ are in increasing order. However, we cannot conclude that at any temperature the cross sections for $\rho\phi \to K\bar{K}$, $\rho\phi \to K\bar{K}^*$ and $\rho\phi \to K^*\bar{K}^*$ at any $\sqrt{s}$ must take the order.

4 Summary

In the Born approximation we have obtained temperature-dependent cross sections for the five nonresonant reactions, $\pi\phi \to K\bar{K}^*$ (or $K^*\bar{K}$), $\pi\phi \to K^*\bar{K}^*$, $\rho\phi \to K\bar{K}$, $\rho\phi \to K\bar{K}^*$ (or $K^*\bar{K}$) and $\rho\phi \to K^*\bar{K}^*$, which are governed by the quark interchange. The numerical cross sections are parametrized and a procedure on how to use the cross sections is given for future applications. The peak cross sections for the endothermic $\pi\phi$ reactions rise or fall with increasing temperature. In addition to the features of exothermic reactions at the threshold energies, the $\rho\phi$ reactions at some temperatures have peak cross sections. At a higher temperature the $\pi\phi$ and $\rho\phi$ reactions are in general more sensitive to the energy variation with respect to the threshold energies. The above in-medium modification to the in-vacuum ϕ absorption is considerable. This is fundamentally related to the temperature dependence of the quark potential, the quark-antiquark wave functions and the meson masses that drop with increasing temperature in consequence of QCD.

Appendix A

The spin-averaged mass of a spin-0 meson and a spin-1 meson with the same isospin is one-fourth of the spin-0 meson mass plus three-fourths of the spin-1 meson mass. The spin-averaged mass is obtained by solving the Schrödinger equation with the central spin-independent potential or by summing the quark mass, the antiquark mass and the nonrelativistic-Hamiltonian expectation value of the quark-antiquark relative-motion wave function. The mass splitting of a spin-0 meson and a spin-1 meson with the same isospin is given by the expectation value of the spin-spin interaction. After the spin-averaged mass and the mass splitting are obtained, we find meson masses of which the mass of the spin-0 meson is the spin-averaged mass minus three-fourths of the mass splitting and the mass of the spin-1 meson is the spin-averaged mass plus one-fourth of the mass splitting. The vacuum masses of pion, rho, kaon and vector kaon are listed in Table 1 of Ref. [19] and the temperature dependence of meson masses in the region $0.6 \leqslant T/T_c \leqslant 0.99$ is shown in Fig. 2 of Ref. [19]. In this temperature region the four meson masses decrease with increasing temperature and the π and ρ masses approach zero at $T \to T_c$. This tendency is consistent with the dropping mass scenarios in Refs. [28, 29]. Parametrizations of the temperature-

dependent masses in units of GeV are

$$m_\pi = 0.41\left[1-\left(\frac{T}{1.05T_c}\right)^{11.88}\right]^{3.81}, \quad \text{(A1)}$$

$$m_\rho = 0.73\left[1-\left(\frac{T}{0.992T_c}\right)^{3.67}\right]^{0.989}, \quad \text{(A2)}$$

$$m_K = 0.634\left[1-\left(\frac{T}{1.105T_c}\right)^{8.646}\right]^{2.591}, \quad \text{(A3)}$$

$$m_{K^*} = 0.84\left[1-\left(\frac{T}{1.05T_c}\right)^{4.16}\right], \quad \text{(A4)}$$

m_π and m_{K^*} are also given by Eqs. (A6) and (A9) in Ref. [19]. m_ρ and m_K displayed here fit the temperature dependence of the ρ and K masses better than Eqs. (A7) and (A8) in Ref. [19].

It is assumed in Ref. [19] that the spatial wave functions of quark-antiquark relative motion of all the mesons in the ground-state pseudoscalar octet and the ground-state vector nonet are identical while the spatial wave functions of π and ρ are a solution of the Schrödinger equation with the central spin-independent potential. Let $\bar{m}_{0\phi}$ denote the spin-averaged mass of the ϕ meson and the $s\bar{s}$ state with spin 0. $\bar{m}_{0\phi}$ equals the nonrelativistic-Hamiltonian expectation value of the ϕ wave function plus two times the strange quark mass. Let $\Delta m_{0\phi}$ denote the mass splitting of the ϕ meson and the $s\bar{s}$ state with spin 0. $\Delta m_{0\phi}$ equals the $V_{s\bar{s}}$ expectation value of the ϕ wave function. We calculate the ϕ mass according to

$$m_\phi = \bar{m}_{0\phi} + \frac{1}{4}\Delta m_{0\phi}. \quad \text{(A5)}$$

Let $\bar{m}_{0\omega}$ be the spin-averaged mass of the ω meson and the $\frac{1}{\sqrt{2}}(u\bar{u}+d\bar{d})$ state with spin 0. $\bar{m}_{0\omega}$ equals the nonrelativistic-Hamiltonian expectation value of the ω wave function plus two times the up quark mass. The masses of the $\frac{1}{\sqrt{6}}(u\bar{u}+d\bar{d}-2s\bar{s})$ states with spins 0 and 1 are m_η and $\frac{1}{3}m_\omega+\frac{2}{3}m_\phi$, respectively. The spin-spin interaction thus yields the mass splitting of the two states, $\Delta m_{\eta\omega\phi} = \frac{1}{3}m_\omega+\frac{2}{3}m_\phi - m_\eta$. From the flavor wave functions of η, ω and ϕ, we have the spin-averaged mass of the two states

$$\frac{1}{4}m_\eta + \frac{3}{4}\left(\frac{1}{3}m_\omega+\frac{2}{3}m_\phi\right) = \frac{1}{3}\bar{m}_{0\omega}+\frac{2}{3}\bar{m}_{0\phi}. \quad \text{(A6)}$$

We finally arrive at the η mass

$$m_\eta = \frac{1}{3}\bar{m}_{0\omega}+\frac{2}{3}\bar{m}_{0\phi}-\frac{3}{4}\Delta m_{\eta\omega\phi}. \quad \text{(A7)}$$

We obtain the vacuum masses of ϕ and η to be 1.0179 GeV and 0.6032 GeV, respectively, compared with the experimental data 1.0195 GeV and 0.5479 GeV. The central spin-independent potential in Eq. (1) has the behavior of $\tanh(Ar)$ at large distances and cannot mimic the linear confinement. In vacuum the ϕ mass is about two times the η mass and the phi is thus not sensitive to the potential behavior at large distances while the eta is a little sensitive to the behavior. Therefore, the ϕ mass is well reproduced while the η mass is approximately reproduced.

We solve the Schrödinger equation with the potential in Eq. (1) to obtain the temperature-dependent quark-antiquark relative-motion wave functions and the masses of ϕ and η are calculated according to Eqs. (A5) and (A7) in the region $0.6 \leqslant T/T_c \leqslant 0.99$ that covers the temperature of hadronic matter. The temperature dependence of ϕ and η masses is shown by the solid and dashed curves in Fig. 6, respectively. Because on the right-hand side of Eq. (1) the first term related to the large-distance behavior of the potential gives a smaller contribution at a higher temperature, the ϕ and η masses decrease with increasing temperature. The masses in units of GeV are parametrized as

$$m_\phi = 0.964\left[1-\left(\frac{T}{1.13T_c}\right)^{5.14}\right]^{1.39}, \quad \text{(A8)}$$

$$m_\eta = 0.691\left[1-\left(\frac{T}{1.21T_c}\right)^{9.067}\right]^{6.029}. \quad \text{(A9)}$$

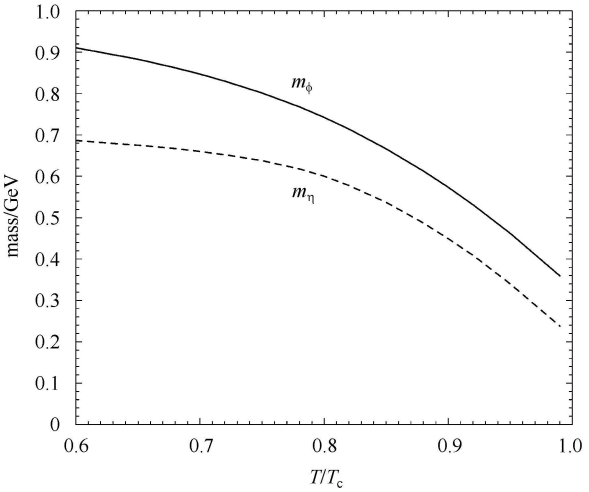

Fig. 6. Meson masses as functions of T/T_c.

Appendix B

The curves shown in Figs. 1–5 correspond to the zero temperature and the five nonzero temperatures $T_1 = 0.65T_c$, $T_2 = 0.75T_c$, $T_3 = 0.85T_c$, $T_4 = 0.9T_c$ and $T_5 = 0.95T_c$. In this appendix we present a procedure on how to obtain unpolarized cross sections for $0.65T_c \leqslant T \leqslant 0.99T_c$ from the curves.

First, we state the procedure for the endothermic $\pi\phi$ reactions. For $T_i \leqslant T \leqslant T_{i+1}(i$=1, 2, 3 or 4) d_0 and $\sqrt{s_z}$ are

$$d_0 = \frac{d_{0i+1}-d_{0i}}{T_{i+1}-T_i}(T-T_i)+d_{0i}, \tag{B1}$$

$$\sqrt{s_z} = \frac{\sqrt{s_{zi+1}}-\sqrt{s_{zi}}}{T_{i+1}-T_i}(T-T_i)+\sqrt{s_{zi}}, \tag{B2}$$

where d_{0i} is d_0 at T_i and $\sqrt{s_{zi}}$ is $\sqrt{s_z}$ at T_i. d_{0i} and $\sqrt{s_{zi}}$ can be found in Tables 1–2. $\sqrt{s_0}$ is the sum of masses of final mesons and parametrizations of the masses have been given by Eqs. (A3) and (A4). The square root of the Mandelstam variable corresponding to the peak cross section is $\sqrt{s_p} = \sqrt{s_0} + d_0$. We define a ratio

$$\zeta = \begin{cases} \dfrac{\sqrt{s}-\sqrt{s_p}}{\sqrt{s_0}-\sqrt{s_p}} & \text{if } \sqrt{s_0} \leqslant \sqrt{s} \leqslant \sqrt{s_p} \\ \dfrac{\sqrt{s}-\sqrt{s_p}}{\sqrt{s_z}-\sqrt{s_p}} & \text{if } \sqrt{s_p} < \sqrt{s} \leqslant \sqrt{s_z}. \end{cases} \tag{B3}$$

The ratio ζ is on the closed interval [0, 1]. The unpolarized cross section for $0.65T_c \leqslant T \leqslant 0.95T_c$ is estimated by

$$\sigma^{\rm unpol}(\sqrt{s},T) = \begin{cases} \dfrac{\sigma_{i+1}-\sigma_i}{T_{i+1}-T_i}(T-T_i)+\sigma_i & \text{if } \sqrt{s_0} \leqslant \sqrt{s} \leqslant \sqrt{s_z} \\ 0 & \text{if } \sqrt{s} > \sqrt{s_z}, \end{cases} \tag{B4}$$

where

$$\sigma_i^{\rm unpol} = \begin{cases} \sigma^{\rm unpol}(\sqrt{s_{pi}}+\zeta(\sqrt{s_{0i}}-\sqrt{s_{pi}}),T_i) & \text{if } \sqrt{s_0} \leqslant \sqrt{s} \leqslant \sqrt{s_p} \\ \sigma^{\rm unpol}(\sqrt{s_{pi}}+\zeta(\sqrt{s_{zi}}-\sqrt{s_{pi}}),T_i) & \text{if } \sqrt{s_p} < \sqrt{s} \leqslant \sqrt{s_z} \end{cases}, \tag{B5}$$

with $\sqrt{s_{pi}}$ being $\sqrt{s_p}$ at T_i and $\sqrt{s_{0i}}$ being $\sqrt{s_0}$ at T_i. $\sigma^{\rm unpol}$ at T_i are the cross sections shown in Figs. 1–2 and are given by Eq. (11) together with the parameters listed in Tables 1–2. For $0.95T_c < T \leqslant 0.99T_c$ Eqs. (B1)–(B5) still apply to obtaining unpolarized cross sections so long as $T_i = T_4$ and $T_{i+1} = T_5$ are set.

Eqs. (B1)–(B3) are suited to endothermic reactions of which each has the zero cross section at the threshold energy and at the infinite center-of-mass energy and has one maximum cross section in its $\sqrt{s}$ dependence. For exothermic reactions cross sections are infinite at threshold energies. But the quantity enclosed by the braces in Eq. (12) has the general $\sqrt{s}$ dependence of endothermic reactions. Hence, Eqs. (B1)–(B3) apply to the quantity enclosed by the braces. $\sqrt{s_0}$ equals the sum of the ρ mass given by Eq. (A2) and the ϕ mass given by Eq. (A8). Eq. (B4) now gives the unpolarized cross sections for exothermic reactions while $\sigma_i^{\rm unpol}$ are the cross sections shown in Figs. 3–5 and are given by Eq. (12) together with the parameters listed in Tables 3–5. Since the infinity of the cross sections at the threshold energies is intractable, do not let $\sqrt{s}$ equal $\sqrt{s_0}$ while fortran code is made.

The above procedure is available for both endothermic and exothermic reactions. It is necessary to apply the procedure to the nonresonant reactions, $\pi\pi \to \rho\rho$ for $I = 2$, $KK \to K^*K^*$ for $I = 1$, $KK^* \to K^*K^*$ for $I = 1$, $\pi K \to \rho K^*$ for $I = 3/2$, $\pi K^* \to \rho K^*$ for $I = 3/2$, $\rho K \to \rho K^*$ for $I = 3/2$ and $\pi K^* \to \rho K$ for $I = 3/2$, for which cross sections at the five nonzero temperatures are given and parametrized in Ref. [19]. Then we list d_0 and $\sqrt{s_z}$ in Tables 6–8 for the seven endothermic reactions. The threshold energy equals the sum of the masses of the two final mesons. d_0 decreases with increasing temperature but becomes a constant or goes up at $T \to T_c$. For readers who are interested in studying in-medium modification by comparing the evolution of mesonic matter at finite temperatures and at the zero temperature, we list a_1, b_1, c_1, a_2, b_2 and c_2 in Table 9 for the seven reactions at $T = 0$. We finally note that we have $a_1 = 0.16$ mb, $b_1 = 0.01$ GeV, $c_1 = 0.56$, $a_2 = 0.08$ mb, $b_2 = 0.07$ GeV and $c_2 = 0.24$ as renewed parameters of the numerical $\rho K \to \rho K^*$ cross sections for $I = 3/2$ at $T/T_c = 0.95$.

Table 6. Values of d_0 and $\sqrt{s_z}$.

T/T_c	$I=2$ $\pi\pi \to \rho\rho$		$I=1$ $KK \to K^*K^*$		$I=1$ $KK^* \to K^*K^*$	
	d_0	$\sqrt{s_z}$	d_0	$\sqrt{s_z}$	d_0	$\sqrt{s_z}$
0	0.2	2.679	0.2251	3.214	0.2251	3.181
0.65	0.1251	1.769	0.1126	2.345	0.1001	2.289
0.75	0.1126	1.416	0.1001	2.114	0.0751	2.086
0.85	0.1126	1.129	0.0686	1.917	0.0626	1.905
0.9	0.0126	0.97	0.0051	1.779	0.0061	1.808
0.95	0.0186	0.889	0.0061	1.663	0.0061	1.705

Table 7. Values of d_0 and $\sqrt{s_z}$.

T/T_c	$I=3/2$ πK → ρK*		$I=3/2$ πK* → ρK*	
	d_0	$\sqrt{s_z}$	d_0	$\sqrt{s_z}$
0	0.2501	3.011	0.2501	2.958
0.65	0.1626	2.166	0.1251	2.109
0.75	0.1251	1.914	0.0936	1.885
0.85	0.0876	1.699	0.0876	1.69
0.9	0.0061	1.548	0.0061	1.58
0.95	0.0126	1.475	0.0126	1.52

Table 8. Values of d_0 and $\sqrt{s_z}$.

T/T_c	$I=3/2$ ρK → ρK*		$I=3/2$ πK* → ρK	
	d_0	$\sqrt{s_z}$	d_0	$\sqrt{s_z}$
0	0.2251	2.876	0.2001	2.552
0.65	0.1126	2.052	0.0251	1.823
0.75	0.0876	1.847	0.0251	1.601
0.85	0.0751	1.678	0.0061	1.273
0.9	0.0061	1.572	0.0061	1.419
0.95	0.0148	1.519	0.0061	1.466

Table 9. Values of parameters at $T=0$.

reaction	a_1/mb	b_1/GeV	c_1	a_2/mb	b_2/GeV	c_2
$I=2$ ππ → ρρ	0.01	0.01	0.39	0.5	0.2	1.48
$I=1$ KK → K*K*	0.01	0.01	0.31	0.61	0.22	1.18
$I=1$ KK* → K*K*	0.01	0.01	0.07	0.95	0.21	1.09
$I=3/2$ πK → ρK*	0.01	0.01	0.51	0.34	0.23	1.36
$I=3/2$ πK* → ρK*	0.01	0.02	0.22	0.49	0.22	1.32
$I=3/2$ ρK → ρK*	0.01	0.01	0.26	0.62	0.21	1.38
$I=3/2$ πK* → ρK	0.01	0.01	0.15	1.25	0.21	1.58

References

1 E917 collaboration. Phys. Rev. C, 2004, **69**: 054901
2 PHENIX collaboration. Phys. Rev. C, 2005, **72**: 014903
3 STAR collaboration. Phys. Rev. C, 2009, **79**: 064903
4 Rafelski J, Müller B. Phys. Rev. Lett., 1982, **48**: 1066
5 Shor A. Phys. Rev. Lett., 1985, **54**: 1122
6 MA Y G. J. Phys. G, 2006, **32**: S373; CHEN J H et al. Phys. Rev. C, 2006, **74**: 064902
7 Molnár D, Voloshin S A. Phys. Rev. Lett., 2003, **91**: 092301
8 PHENIX collaboration. Phys. Rev. Lett., 2003, **91**: 182301
9 Yamamoto E. (STAR collaboration). Nucl. Phys. A, 2003, **715**: 466
10 NA60 collaboration. Eur. Phys. J. C, 2009, **64**: 1
11 PHENIX collaboration. Phys. Rev. C, 2011, **83**: 024909
12 LI Y Q, XU X M, GE H J. Eur. Phys. J. A, 2011, **47**: 65
13 BI P Z, Rafelski J. Phys. Lett. B, 1991, **262**: 485
14 Ko C M, Seibert D. Phys. Rev. C, 1994, **49**: 2198
15 Haglin K. Nucl. Phys. A, 1995, **584**: 719; Smith W, Haglin K L. Phys. Rev. C, 1998, **57**: 1449
16 Alvarez-Ruso L, Koch V. Phys. Rev. C, 2002, **65**: 054901
17 LI Y Q, XU X M. Nucl. Phys. A, 2007, **794**: 210
18 Barnes T, Swanson E S. Phys. Rev. D, 1992, **46**: 131; Swanson E S. Ann. Phys. (N.Y.), 1992, **220**: 73
19 ZHANG Y P, XU X M, GE H J. Nucl. Phys. A, 2010, **832**: 112
20 Buchmüller W, Tye S-H H. Phys. Rev. D, 1981, **24**: 132
21 Karsch F, Laermann E, Peikert A. Nucl. Phys. B, 2001, **605**: 579
22 WONG C Y. Phys. Rev. C, 2002, **65**: 034902
23 Digal S, Petreczky P, Satz H. Phys. Lett. B, 2001, **514**: 57
24 XU X M. Nucl. Phys. A, 2002, **697**: 825
25 Mott N F, Massey H S W. The Theory of Atomic Collisions. Oxford: Clarendon Press, 1965
26 Barnes T, Black N, Swanson E S. Phys. Rev. C, 2001, **63**: 025204
27 WONG C Y, Crater H W. Phys. Rev. C, 2001, **63**: 044907
28 Weinberg S. Phys. Rev. Lett., 1990, **65**: 1177
29 Brown G E, Lee C H, Rho M. Phys. Rev. C, 2006, **74**: 024906